Temperature-insensitivity gas pressure sensor based on inflated long period fiber grating inscribed in photonic crystal fiber

Xiaoyong Zhong, Yiping Wang,* Changrui Liao, Shen Liu, Jian Tang, and Qiao Wang

Key Laboratory of Optoelectronic Devices and Systems of Ministry of Education and Guangdong Province,
College of Optoelectronic Engineering, Shenzhen University, Shenzhen 518060, China
*Corresponding author: ypwang@szu.edu.cn

We demonstrated an inflated long period fiber grating (I-LPFG) inscribed in a pure-silica photonic crystal fiber (PCF) for high-sensitivity gas pressure sensing applications. The I-LPFG was inscribed by use of the pressure-assisted CO_2 laser beam-scanning technique to inflate periodically air holes of a PCF along the fiber axis. Such an I-LPFG with periodic inflations exhibits a very high gas pressure sensitivity of 1.68 nm/MPa, which is one order of magnitude higher than that, i.e., 0.12 nm/Mpa, of the LPFG without periodic inflations. Moreover, the I-LPFG has a very low temperature sensitivity of 3.1 pm/°C due to the pure silica material in the PCF so that the pressure measurement error, resulting from the cross-sensitivity between temperature and gas pressure, is less than 1.8 Kpa/°C in the case of no temperature compensation. So the I-LPFG could be used to develop a promising gas pressure sensor, and the achieved pressure measurement range is up to 10 MPa.   © 2015 Optical Society of America

OCIS codes: (060.5295) Photonic crystal fibers; (050.2770) Gratings; (060.2340) Fiber optics components; (060.2370) Fiber optics sensors.

http://dx.doi.org/10.1364/OL.40.001791

Over the past decade, various kinds of fiber optic gas pressure sensors such as Fabry–Perot interferometers (FPIs) [1–4], fiber Bragg gratings (FBGs) [5–8], and long-period fiber gratings (LPFGs) [9–12] have been extensively investigated and been widely used in the field of industrial and environmental monitoring. Among them, LPFG-based gas-pressure sensors are of great interest owing to their easy fabrication, compact size, low cost, robustness, and immunity to electro-magnetic interference. Unfortunately, gas-pressure sensitivity of LPFG was usually very low, e.g., only 5.1 pm/bar in a Corning SMF-28 fiber [13] and 11.2 pm/bar in a photonic crystal fiber (PCF) [14], respectively. In addition, during the applications of LPFG-based gas pressure sensors, one of the main difficulties is the cross-sensitivity between the gas pressure and the temperature. For instance, the gas-pressure sensor based on a LPFG written in a SMF-28 fiber [13] and a boron codoped optical fiber [15] exhibited a temperature sensitivity of 49.5 pm/°C and 0.72 nm/°C, respectively. Hence, the cross-sensitivity of the LPFG-based sensors limits their applications in the field of practical gas pressure monitoring.

In this report, we demonstrated the inscription of an inflated long-period fiber grating (I-LPFG) in a PCF by means of the pressure-assisted CO_2 laser beam-scanning technique to inflate periodically air holes along the fiber axis. Such an I-LPFG sensor exhibited a high gas-pressure sensitivity of up to 1.68 nm/Mpa, which is one order of magnitude higher than that reported previously in ref. [14]. The novel I-LPFG also exhibited an intensity-modulated gas-pressure sensitivity of 1.36 dB/Mpa. Moreover, a low temperature sensitivity of 3.1 pm/°C was achieved in the I-LPFG-based gas-pressure sensor, which can effectively reduce the cross-sensitivity between gas pressure and temperature.

An experiment setup, as shown in Fig. 1 reported in Ref. [16], was employed to write an inflated long-period

fiber grating (I-LPFG) by use of the pressure-assisted CO_2 laser beam-scanning technique to inflate periodically air holes of a PCF along the fiber axis. The pressure, P_s, required to avoid collapsing a hole in a PCF is related to the surface tension, γ, of the hole, which can be expressed as [17]

$$P_s = 2\gamma/d, \qquad (1)$$

where d is the hole diameter. For a given d and internal gas pressure P, the hole in a PCF will either inflate or collapse depending on whether P is higher or lower than P_s during CO_2 laser irradiation. And the rate of the hole inflation or collapse depends on the temperature of the glass and the magnitude of the pressure P. For an inflated
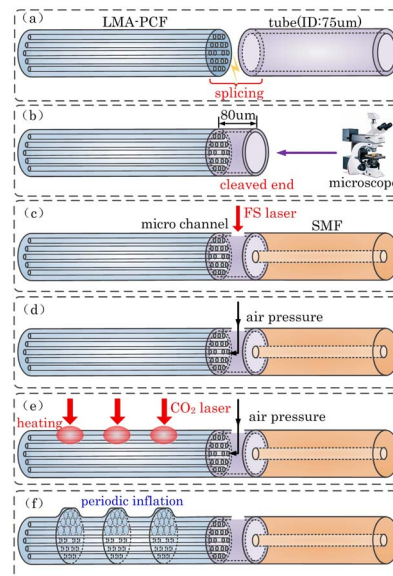

Fig. 1.   Schematic diagram for fabricating an I-LPFG sensor.

© 2015 Optical Society of America

grating, the main design parameters are the internal gas pressure, CO_2 laser power, and exposure time. In our experiment, the internal gas pressure was about 1.5 MPa, the output power of the CO_2 laser was 0.4 W, and the average exposure time was 200 ms.

Figure 1 illustrates the detailed process for fabricating an I-LPFG-based sensor. First, as shown in Fig. 1(a), an end of a silica tube with an inner/outer diameter of 75/127 µm was spliced with a large-mode-area pure-silica PCF (NKT ESM-12) by use of a commercial fusion splicer (FSM-60) in the manual mode. Note that the discharge current of the splicer must be manually adjusted to avoid collapsing of the air holes at the splicing joint so that air can pass through the silica tube into the holes of the PCF, as described below. Second, as shown in Fig. 1(b), another end of the silica tube was cleaved to shorten its length to be about 80 µm so that we can observe whether the air holes of the PCF end are open or not by use of a microscope. Third, as shown in Fig. 1(c), the cleaved end of the silica tube was spliced with another single-mode fiber (SMF), thus achieving an air cavity with a length of 80 µm. And then a micro-channel (50*40 µm) was drilled through the sidewall of the silica tube by use of a femtosecond laser (a central wavelength of 800 nm, a pulse duration time of 120 fs, and a repetition rate of 1 kHz) so that air pressure can access from the silica tube into the air holes of the PCF. Fourth, as shown in Fig. 1(d), the silica tube with a channel was placed into a gas chamber and sealed by use of strong glue. Then air with a pressure of ~1.5 MPa accessed the holes of the PCF via the gas chamber by use of a high-pressure air pump. Finally, as shown in Figs. 1(e) and 1(f), the PCF was periodically heated along the fiber axis by use of a focused CO_2 laser beam. As a result, the holes of the PCF inflated periodically along the fiber axis due to high-pressure air and the CO_2-laser-induced high temperature. Such inflations induce periodically refractive index modulation along the fiber axis, thus inscribing an I-LPFG in the PCF, as shown in Fig. 2. Periodical heating process, i.e., the so-called scanning cycle above, may be repeated for K cycles from the first grating period to the last grating period until a desired I-LPFG is achieved, as shown in Fig. 3.

As shown in Fig. 2 (a), air holes of a PCF employed with a diameter of 3.3 µm are arranged in a hexagonal pattern with a pitch of 7.4 µm. The core and cladding diameters of the PCF are 10.4 and 125 µm, respectively. As shown in Figs. 2(b) and 2(c), asymmetric inflations of
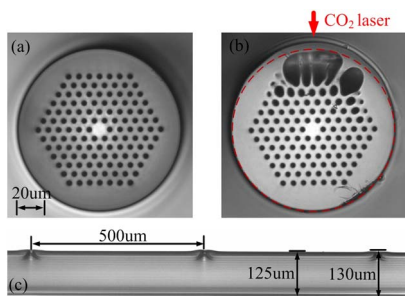

Fig. 2. Microscope image of the cross-section of the PCF (a) before and (b) after CO_2 laser irradiation, (c) side view of the CO_2-laser-inscribed I-LPFG with periodic inflations.
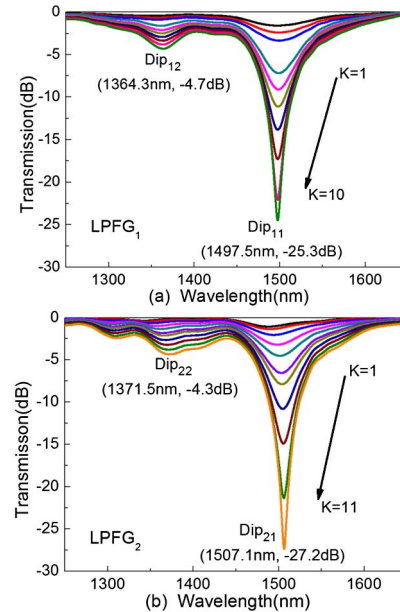

Fig. 3. Transmission spectrum evolution of the CO_2-laser-inscribed (a) $LPFG_1$ with periodic inflations and (b) $LPFG_2$ without periodic inflations while the number of scanning cycles (K) increases.

air holes were clearly created in the PCF along the fiber axis, resulting from the single-side irradiation of the focused CO_2 laser beam. Compared with the PCF diameter of 125 µm, the inflated region of the PCF has a diameter of 130 µm along the CO_2 laser irradiation direction. Uneven expansion of the air holes illustrated in Fig. 2(b) may be due to the inhomogeneity of the air holes in the PCF.

As shown in Fig. 3(a), a high-quality I-LPFG sample, i.e., $LPFG_1$, with asymmetric periodic inflations, a low insertion loss of ~1 dB, and two attenuation dips (Dip_{11} and Dip_{12}) were induced after ten scanning cycles of the CO_2 laser beam, where the resonant wavelengths and the attenuation dips of Dip_{11} and Dip_{12} are $\lambda_{11} = 1497.5$ nm, $A_{11} = -25.3$ dB, $\lambda_{12} = 1364.3$ nm, and $A_{12} = -4.7$ dB, respectively.

To observe the difference between the gas pressure response of the LPFGs with and without periodic inflations, another LPFG sample, i.e., $LPFG_2$, without periodic inflations was inscribed in the same type of PCF by means of the common CO_2 laser irradiation technology [18], in which no high-pressure air was pumped into the air holes of the PCF. During the inscription of $LPFG_2$, a lower power of the CO_2 laser was employed to avoid collapsing of the air holes of the PCF [19]. As shown in Fig. 3(b), the insertion loss of ~0.8 dB and two attenuation dips (Dip_{21} and Dip_{22}) were observed in the transmission spectrum of $LPFG_2$ after eleven scanning cycles of the CO_2 laser beam, where the resonant wavelengths and the attenuation dips of Dip_{21} and Dip_{22} are $\lambda_{21} = 1507.1$ nm, $A_{21} = -27.2$ dB, $\lambda_{22} = 1371.5$ nm, and $A_{22} = -4.3$ dB, respectively. $LPFG_1$ and $LPFG_2$ are with the same grating pitch of 500 µm and the same period numbers of 30.

An experimental setup for investigating the responses of the LPFG samples to gas pressure is illustrated in Fig. 4, where a broadband light source (BBS) and an
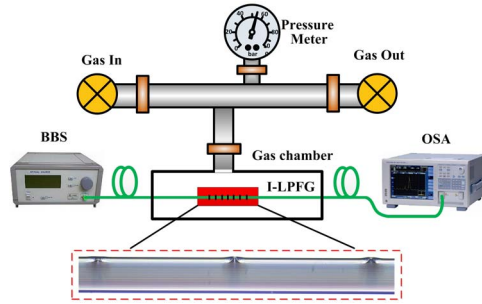
Fig. 4. Experimental setup for investigating the response of the LPFG samples to the gas pressure.

optical-spectrum analyzer (OSA) with a resolution of 0.01 nm were employed to measure the transmission spectra of the gratings. The LPFG samples, i.e., LPFG$_1$ with periodic inflations or LPFG$_2$, without periodic inflations was sealed in a gas chamber by use of a strong glue, where a commercial air pump was used to realize air pressure measurement via a high-precision pressure meter (ConST-162) with a pressure range from up to 40 MPa.

Resonant wavelength of each LPFG sample was measured while the gas pressure in the chamber was increased from 0 to 10 MPa with a step of 1 Mpa, remaining for 10 min at each step. With the increase of gas pressure, as shown in Figs. 5 and 6(a), the resonant wavelength of LPFG$_1$ with periodic inflations, i.e., I-LPFG, shifted rapidly toward a longer wavelength with a higher sensitivity of 1.68 nm/Mpa, whereas, that of LPFG$_2$ without periodic inflations shifted slowly toward a longer wavelength with a lower sensitivity of 0.12 nm/Mpa. Moreover, with the increase of gas pressure, as shown in Figs. 5 and 6(b), the attenuation dip of LPFG$_1$ reduced rapidly with a higher sensitivity of 1.36 dB/Mpa, whereas, that of LPFG$_2$ reduced slowly with a lower sensitivity of 0.25 dB/Mpa.

It is obvious that the gas pressure sensitivity of resonant wavelength of LPFG$_1$ with periodic inflations is one order of magnitude higher than that of resonant
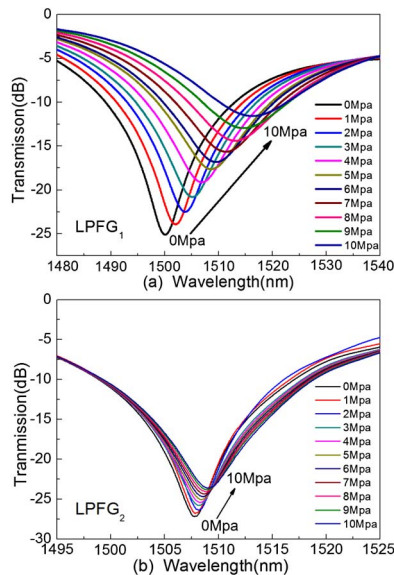
wavelength of LPFG$_2$ without periodic inflations. In other words, the gas pressure sensitivity of the PCF-based LPFG is increased by 14 times by means of inflating periodic air holes of the PCF along the fiber axis. Moreover, the gas pressure sensitivity of our I-LPFG is one order of magnitude higher than that of the taper-induced LPFG in the same type PCF [14]. In terms of an intensity-based measurement, as shown in Fig. 6(b), our I-LPFG sensor exhibits a high pressure sensitivity of 1.36 dB/Mpa, which is much higher than that, i.e., 0.25 dB/Mpa, of LPFG without periodic inflations.

The sensitivity of resonant wavelength, λ_i, of a LPFG to the gas pressure, P, can be defined as follows [13]:

$$\frac{d\lambda_i}{dP} = \Lambda \frac{d(\delta n_{\mathrm{eff},i})}{dP} + \lambda_i \frac{1}{L}\frac{dL}{dP}, \qquad (2)$$

where Λ is the grating pitch, L is the length of the grating, and $\delta n_{\mathrm{eff},i}$ is the effective refractive index difference between the core and the cladding. It is very difficult to analyze quantitatively the pressure sensitivity of the I-LPFG because the inflation of air holes is uneven and irregular. Therefore, we only analyzed qualitatively the increased pressure sensitivity of the I-LPFG in comparison to a conventional LPFG. It has been found that the second term on the right side of Eq. (2) does not play an important role because dL/dP can be neglected in the case of radial pressure. Thus, the resonant wavelength of our I-LPFG sensor is a linear function of the gas pressure, and the gas pressure sensitivity mainly depends on the fiber materials, i.e., the elasto-optical coefficient of the glass and the pressure-induced physical deformations of the fiber. The resonant wavelength shift of our I-LPFG sensor
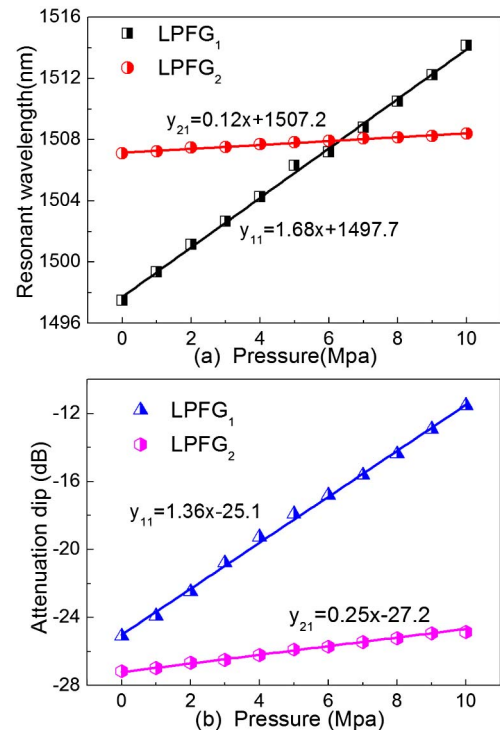

Fig. 5. Transmission spectrum evolution of (a) LPFG$_1$ with periodic inflations and (b) LPFG$_2$ without periodic inflations while the gas pressure increases from 0 to 10 MPa.

Fig. 6. (a) Measured resonant wavelength and (b) attenuation dip of the two LPFG samples, i.e., LPFG$_1$ and LPFG$_2$, versus gas pressure.
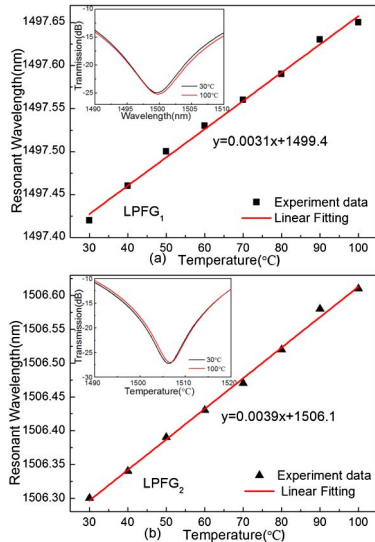
Fig. 7. Temperature responses of (a) the I-LPFG sample, i.e., $LPFG_1$ with periodic inflations and (b) the LPFG sample, i.e., $LPFG_2$ without periodic inflations. Inset: transmission spectra of the LPFG samples at 30°C and 100°C.

is a linear function of the gas pressure, which has been verified by our experimental results illustrated in Fig. 6. Moreover, the silica walls within the inflated region of the I-LPFG are thinned due to the inflation of air holes in the PCF. As a result, in the case of a high gas pressure, physical deformations easily occur within the inflated region of the I-LPFG, which changes the effective refractive index difference, i.e., $\delta n_{\text{eff},i}$ in Eq. (2), due to the well-known elasto-optical effect and induces a resonant wavelength shift. Thus periodic inflations in the I-LPFG greatly enhance the pressure sensitivity of the grating. So our I-LPFG could be used to develop a promising gas pressure sensor with a high sensitivity of up to 1.68 nm/MPa.

We also investigated the temperature response of the I-LPFG by means of placing $LPFG_1$ into an electrical oven and raising gradually the temperature from room temperature to 100°C with a step of 10°C. The tested temperature was maintained for 20 min at each temperature rise step. As shown in Fig. 7(a), the resonant wavelength of the I-LPFG with periodic inflations was shifted toward a longer wavelength with a low sensitivity of 3.1 pm/°C. In other words, the I-LPFG based sensor is insensitive to temperature. The reason for this is that the I-LPFG was induced in a pure-silica PCF. For a comparison, we also investigated the temperature response of the LPFG sample, i.e., $LPFG_2$, without periodic inflations. As shown in Fig. 7(b), the resonant wavelength of the $LPFG_2$ was also shifted toward a longer wavelength with a low sensitivity of 3.9 pm/°C. It can be seen from Fig. 7 that the temperature sensitivity of $LPFG_1$ is similar to that of $LPFG_2$. Thus the inflations of air holes in a PCF have little influence on the temperature sensitivity in a low-temperature test. According to the pressure and temperature sensitivities above, proving the I-LPFG is used to measure gas pressure, the pressure measurement error, resulting from the cross-sensitivity between temperature and gas pressure, is less than 1.8 Kpa/°C, which could be neglected in high gas-pressure measurement. Therefore, our I-LPFG pressure sensor could effectively reduce

the cross-sensitivity between gas pressure and temperature.

In conclusion, we have experimentally demonstrated a novel I-LPFG for high-sensitivity gas-pressure measurement. Such an I-LPFG was induced by use of a pressure-assisted CO_2 laser beam-scanning technique to inflate periodically air holes of a PCF. A very high-pressure sensitivity of 1.68 nm/Mpa was achieved, which is increased by 14 times, comparing with that of the LPFG without periodic inflations. Moreover, the I-LPFG exhibited a very low-temperature sensitivity of 3.1 pm/°C so that the pressure measurement error, resulting from the cross-sensitivity between temperature and gas pressure, is less than 1.8 Kpa/°C in the case of no temperature compensation. So the I-LPFG could be used to develop a promising gas-pressure sensor, and the achieved pressure measurement range is up to 10 MPa.

References

1. C. A. Wu, H. Y. Fu, K. K. Qureshi, B. O. Guan, and H. Y. Tam, Opt. Lett. **36**, 412 (2011).
2. J. Ma, W. Jin, H. L. Ho, and J. Y. Dai, Opt. Lett. **37**, 2493 (2012).
3. Y. N. Zhang, L. Yuan, X. W. Lan, A. Kaur, J. Huang, and H. Xiao, Opt. Lett **38**, 4609 (2013).
4. C. R. Liao, S. Liu, L. Xu, C. Wang, Y. P. Wang, Z. Y. Li, Q. Wang, and D. N. Wang, Opt. Lett. **39**, 2827 (2014).
5. T. Chen, R. Z. Chen, C. Jewart, B. T. Zhang, K. Cook, J. Canning, and K. P. Chen, Opt. Lett. **36**, 3542 (2011).
6. C. M. Jewart, Q. Q. Wang, J. Canning, D. Grobnic, S. J. Mihailov, and K. P. Chen, Opt. Lett. **35**, 1443 (2010).
7. H. J. Sheng, W. F. Liu, K. R. Lin, S. S. Bor, and M. Y. Fu, Opt. Express **16**, 16013 (2008).
8. Q. Zhang, N. Liu, T. Fink, H. Li, W. Peng, and M. Han, IEEE Photon. Technol. Lett. **24**, 1519 (2012).
9. G. Statkiewicz-Barabach, D. Kowal, M. K. Szczurowski, P. Mergo, and W. Urbanczyk, IEEE Photon. Technol. Lett. **25**, 496 (2013).
10. Y. F. Zhang, C. C. Chan, Y. M. Chan, and P. Zu, IEEE Sens. J. **12**, 954 (2012).
11. M. Smietana, W. J. Bock, P. Mikulic, and J. H. Chen, J. Lightwave Technol. **30**, 1080 (2012).
12. Y. Wang, J. Appl. Phys. **108**, 081101 (2010).
13. W. J. Bock, J. Chen, P. Mikulic, and T. Eftimov, IEEE Trans. Instrum. Meas. **56**, 1176 (2007).
14. W. J. Bock, J. Chen, P. Mikulic, T. Eftimov, and M. Korwin-Pawlowski, Meas. Sci. Technol. **18**, 3098 (2007).
15. M. Smietana, W. J. Bock, J. Chen, and P. Mikulic, Meas. Sci. Technol. **21**, 094026 (2010).
16. X. Y. Zhong, Y. P. Wang, J. L. Qu, C. R. Liao, S. Liu, J. Tang, Q. Wang, J. Zhao, K. M. Yang, and Z. Y. Li, Opt. Lett. **39**, 5463 (2014).
17. W. J. Wadsworth, A. Witkowska, S. G. Leon-Saval, and T. A. Birks, Opt. Express. **13**, 6541 (2005).
18. Y. Zhu, P. Shum, H. W. Bay, M. Yan, X. Yu, J. Hu, J. Hao, and C. Lu, Opt. Lett. **30**, 367 (2005).
19. Y. P. Wang, L. M. Xiao, D. N. Wang, and W. Jin, Opt. Lett. **31**, 3414 (2006).